Predicting the Age of Healthy Adults from Structural MRI by Sparse Representation

Longfei Su, Lubin Wang, and Dewen Hu*

College of Mechatronics and Automation
National University of Defense Technology
Changsha, Hunan 410073, China
dwhu@nudt.edu.cn

Abstract. It is generally accepted that degenerative brain diseases lead to abnormal aging process of the human brain. Thus, healthy brain aging model has great potential in clinical diagnosis and intervention. The aim of this work is to construct a regression model which is efficient for age prediction of healthy brain. Two groups of T1-weighted MRI images were involved. The first group was used for voxel selection then corresponding voxels in the second group were used for age prediction. Then mean absolute error (MAE) between the predicted age and the true age is obtained. The age prediction accuracy can reach as high as 4.67 years (MAE). In conclusion, the framework in current study can be a healthy aging model for abnormality detection of human brain. The brain regions identified by this model is sensitive to aging process which can be viewed as biomarker of brain age.

Keywords: healthy brain aging, age prediction, MRI; voxel selection, MAE, biomarker of brain age.

1 Introduction

Population aging-the older individuals become larger percentage of the total population - is a worldwide problem which will be faced by all the countries. Try our best to keep the elderly healthy is of ultimate importance. Aging research is now gaining momentum. Cognitive decline or dementia is one of the greatest health threats to the elders. Old age itself is the biggest risk factor for these neurodegenerative disease [1]. Hypothesis that some neurodegenerative diseases are accelerated aging process is supported by some previous studies [2-5]. Through comparing the chronological age and the predicted brain age, early diagnose of the pathologic brain abnormality before the onset of clinical symptoms is enabled. Efficient, reliable and robust methods are urgently called for age prediction of healthy brain.

Based on GM of structural MRI images, researchers took use of the framework of hidden Markov models for age prediction and got a high accuracy (MAE: 2.16 years for

* Corresponding author.

J. Yang, F. Fang, and C. Sun (Eds.): IScIDE 2012, LNCS 7751, pp. 271–279, 2013.
© Springer-Verlag Berlin Heidelberg 2013

8 healthy subjects, age: 50-76 years; MAE: 2.41 years for 20 healthy subjects, age 50-86 years), but the sample size is too small [6]. Even higher age prediction accuracy was achieved (MAE: about 1 year), but the subject age range is 3 to 20 years [7]. Principle component analysis (PCA) and relevance vector regression (RVR) were both used for age prediction based on T1-weighted MRI images [4]. High prediction accuracy was achieved - mean absolute error (MAE) is 4.98 years. This confirms the predictive ability of T1-weighted MRI images. But, components obtained from PCA method consist of information from all the features (voxels).

It is universally accepted that human brain shrinks with age. For main reason of whole brain age-related volume decline is the decrease of GM volume [8], study about age effects on GM has a unique position in this field [9,10]. Most white matter (WM) changes occur during advanced aging process, but GM seems to be a constant, linear function of age [11-14]. VBM studies estimate that loss of GM is 0.18% per year [15]. Age-related changes are too subtle to be detected and lead to different even controversial conclusion. Thus, we need new technique to mine the implicit age information from MRI.

Currently, in the face of the problem named overfitting – that is too complex relationship will be established when too many features were involved which will lead to poor generalization. Many studies have confirmed that only part of the features were useful for classification or prediction [16-18]. And, sufficient evidence have shown that sparsity is promising in MRI studies [19]. Here, a feature selection method based on sparse representation was employed to select the most discriminative voxels for age prediction.

Combining of the sparse representation voxel selection and RVR, we predict the brain age of the subjects based on their T1-weighted MRI images.

2 Materials and Methods

2.1 Participants

This study's participants were selected from two databases. One group included 290 healthy subject's images which were available at the open access series of imaging studies (OASIS) website (http://www.oasis-brains.org). The initial data set in OASIS consists of a cross-sectional collection of 416 subjects with detailed description in [20]. One hundred subjects suffered with Alzheimer disease (AD) and 26 with excessive head motion were removed.

The second group consisted of eighty four healthy volunteers participated in this study. All of the subjects were left-handed except two were ambidextrous and four were left-handed. Characteristics of the two groups of subjects are displayed in Table 1.

Table 1. Characterization of subjects in this study

Variable	Group 1	Group 2
Sample size	290	84
Age (mean ± SD years)	43.25 ± 23.04	43.98 ± 17.38
Gender (male/female)	107/183	41/43
Age range (years)	18-91	19-79

2.2 Imaging Protocol

For group 1, T1-weighted structural magnetization prepared rapid gradient echo (MP-RAGE) images were obtained with the following parameters: TR = 9.7 ms, TE = 4 ms, slice thickness = 1.25 mm, flip angle = 10°, and in-plane resolution = 256 × 256 (1 mm × 1 mm). For each subject, 3-4 T1-weighted structural images were obtained on a 1.5 T Vision scanner (Siemens, Erlangen, Germany) during a single image session. In this study, one T1-weighted MRI image was selected randomly for each subject. For group 2, the T1-weighted structural MRI images were acquired with the following parameters: TR = 22 ms, TE = 9.2 ms, slice thickness = 1 mm, flip angle = 30° and in-plane resolution = 256 × 256 (1 mm × 1 mm). All scans were performed on the same Siemens Sonata 1.5 T MRI scanner.

2.3 Data Preprocessing

Data preprocessing was performed using SPM8 toolbox (http://www.fil.ion.ucl.ac.uk/spm/). First, the new segment procedure was used to segment the MRI images into GM, WM, cerebrospinal fluid (CSF) and three other background partitions. Next, one template was generated from each group of dataset using the diffeomorphic anatomical registration by exponentiated Lie algebra (DARTEL) technique [21] which matched the GM and WM to each other. Finally, GM images were spatially normalized to the template that was created in the second step and then smoothed by an isotropic Gaussian filter with an 8 mm full-width half-maximum kernel.

2.4 Voxel Selection

The proposed voxel selection method includes two steps: the t-test filter and the sparse representation algorithm. In order to achieve cluster effect and fix the computational problem faced by sparse representation algorithm, we filtered the original data by t-test and retained 20000 voxels in the first step. Then in the second step, the sparse representation algorithm was performed on the retained voxels. The purpose of the first step is to select voxels by considering the relationship between single voxel and age,

while the second step aimed at selecting bundle of voxels based on the accumulating information contained in covarying relationship of voxels in different location [22]. Details of the sparse representation algorithm are shown below.

1. For $t = 1, 2, ..., T$, (in this study, we choose $T = 200$ empirically) perform steps 2 to 4.
2. Using matrix $A^t, (A^1 = A)$, and the label y (age), perform steps 2.1-2.2 for $k = 1, 2, ..., R$ times (in this study, we choose $R = 300$ empirically).

   2.1: Randomly choose $q = 0.1n$ (n = rows of A) rows from A^t to a construct submatrix A_k, corresponding q entries of y forms y_k.

   2.2: Solve optimization problem

$$min \|w\|_1, \ subject \ to \ A_k w = y_k \tag{1}$$

   We denote the solution of equation S.1 as w^k.

3. Let

$$w = \left| \frac{1}{300} \sum_{k=1}^{300} w^k \right| \tag{2}$$

4. According the weight vector w, the 100 voxels with highest elements are selected. Column index of these 100 voxels are defined as ind^t. After these 100 columns removed from A^t, the remaining columns form A^{t+1}.
5. $[ind^1, ind^2, ..., ind^T]$ is the new rearranged index of the 20000 voxels.

2.5 Age Prediction and Validation

RVR was used for regression. In this study, 10-fold cross validation for group 1, leave one out cross validation for group 2 was used to confirm the prediction accuracy.

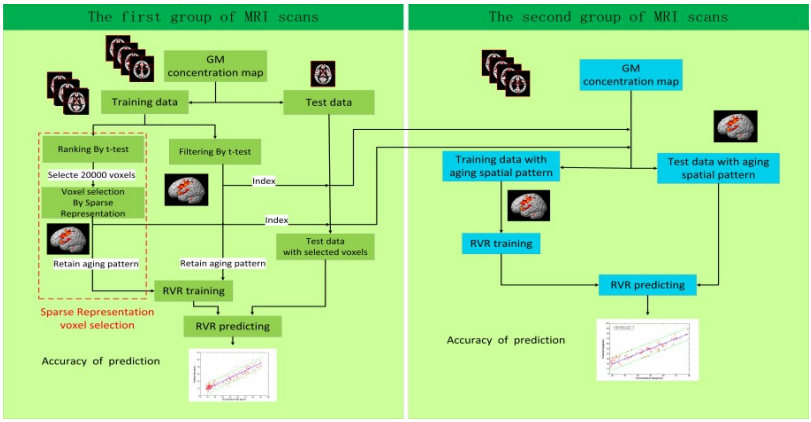

Fig. 1. Procedure of voxels selection and regression for age prediction

The first 1200 voxels in the intersection among the ten groups of rearranged voxels were chosen as the final aging spatial patterns. To confirm the robustness of the sparse representation method, we applied the spatial patterns of aging that were selected from the first group of MRI images to the second group of MRI images for age prediction. The voxels selection and the regression procedure are illustrated in Fig. 1.

3 Results

3.1 Results of the First Group of MRI Scans

For the first group of MRI scans (down load from website: http://www.oasis-brains.org) contain more young subjects especially the subjects aged 20 to 30 than other age steps, so in our results of Fig 2 more points concentrated in the 20-30 range. Voxel selection and the age prediction using RVR were all go through the ten-fold cross-validation. The voxel selection step consists of t-test filter and sparse representation based voxel selection. As a comparison, the 1200 voxels selected by our voxel selection method and the 1200 voxels selected by only the t-test filter were separately used for age prediction. The results were both shown in Fig 2. The left panel is the age prediction results using our voxel selection method; the right is the results using t-test filter. We take use of mean absolute error (MAE) and standard deviation (SD) to evaluate the performance of the two age prediction models. The age prediction results of the two models are both shown in Table 2.

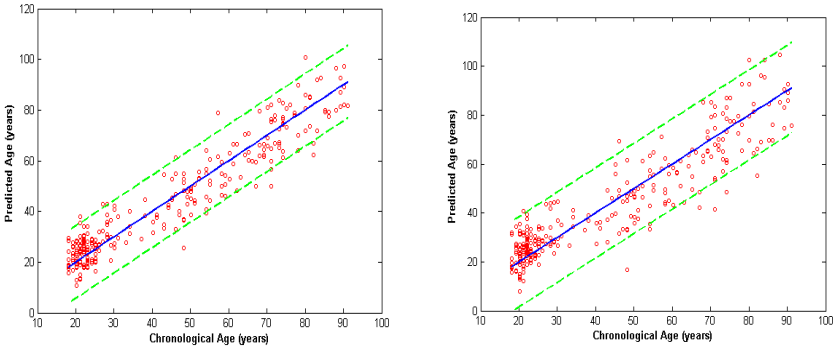

Fig. 2. Age prediction results of the first group of MRI scans. The left panel is the results corresponding to our method; the right panel is the results corresponding to t-test + RVR. Chronological age is shown on the x-axis and predicted age on the y-axis. Correctly prediction is shown by solid blue line, 95% predictions limits are shown in dash green lines.

Table 2. Age prediction accuracy of the presented method and the t-test + RVR in group 1

Group 1	MAE （years）	SD(years)
t-test + Sparse representation	5.69	7.15
t-test + RVR	6.93	9.23

From Fig 2 and Table 2 we can see that our voxel selection method was more efficient for age prediction than the t-test method. Not only the MAE but also the SD of our method is lower than the t-test method, which means our method can explore more age information and the selected biomarker is more stable and robust. But, due to the ten-fold cross-validation, the 1200 voxels in one fold were not completely identical to the 1200 voxels of the other fold. So, it cannot extract a general, stable and accurate biomarker for human brain aging. To fix this problem, we reevaluated the selected voxels in more wide range and identified the common voxels shared by all the ten folds. Then we get the final aging biomarker. For the final biomarker contain aging information of all the scans in the first group, we had to test it on another group of MRI scans.

3.2 Results of the Second Group of MRI Scans

According the index of the final biomarker obtained from the first group of MRI images, we select 1200 voxels as the input of the RVR. Using only these voxels, we successfully predicted the age of the subjects. The prediction results were more accurate than the results of first group. The details were all displayed in Table 3.

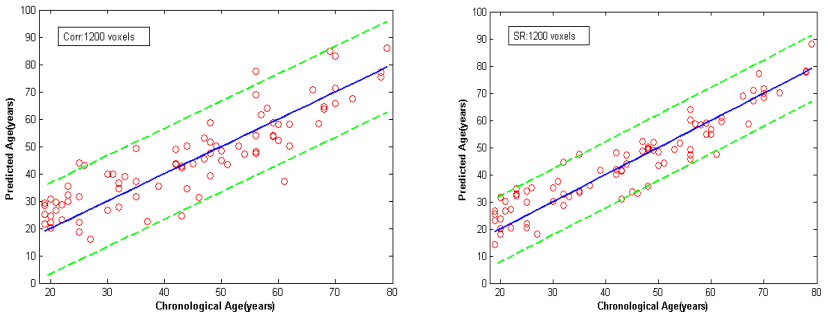

Fig. 3. Age prediction results of the second group of MRI scans. Different from Fig. 2, this results used the final biomarker extracting from the first group of MRI scans.

Table 3. Age prediction accuracy of the presented method and the t-test + RVR in group 2

Group 2	MAE(years)	SD(years)
t-test + Sparse representation +	4.67	6.10
t-test + RVR	6.54	8.33

Compare Table 3 with Table 2 we can see that the final biomarker of the human brain aging significantly increased the accuracy of the age prediction. Especially our new voxel selection method, the MAE and SD both declined.

3.3 Biomarker of Human Brain Aging

The 1200 voxels were selected by our method as the biomarker of human brain aging. The results were all shown in Fig 4.

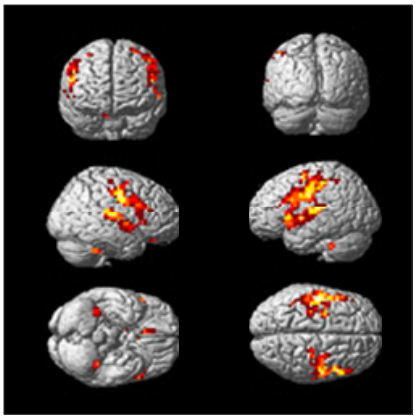

Fig. 4. Biomarker identified by our age prediction model

4 Discussion

In this paper, we presented a sparse representation based model to predict the brain age of the subject using T1-weighted MRI scans. Compare with previous study, our method increased the prediction accuracy and can further identify the most significant brain regions for age prediction.

There is a problem that both using all voxels and dimension reduction by PCA took use of the whole brain aging information, so the discriminative ability of different brain regions cannot be identified. In our model for age prediction, through voxel selection by sparse representation we used only the most discriminative voxels which only a small part of the whole brain voxels. By using only these few voxels, we got an even high accuracy of age prediction (MAE: 4.67 years, SD: 6.10 years). This confirmed the superiority of our age prediction model. From the aspect of physiological interpretation, identification of the aging brain regions is promising in diagnosis of neurodegenerative disease. Related work has also been reported [2-5,23,24].

The brain regions used for age prediction were also identified in this study. The most discriminative voxels were focus on the precentral and postcentral sulci, the medial temporal lobe, the caudate, the right inferior frontal regions, and the cerebellum. This result is highly consistent with our previous study which used sparse representation based voxel selection for age-related classification [18,25]. The difference between voxel selection for age prediction and for age-related classification is the label used in sparse representation algorithm. For classification the label is class information (1 or -1), but for age prediction, the label is the age information (age of subject). However, the results were almost the same. There were also many other studies reported similar

results [26], which confirmed our voxel selection results. So, the regions identified by our method are reliable which can be recognized as biomarker of brain aging.

In conclusion, our new sparse representation based age prediction model can identify the biomarker of brain aging with highly age prediction accuracy. This healthy age prediction model has potential clinical use in early diagnosis of neurodegenerative disease such as AD before onset of clinical symptom.

Acknowledgments. This work was supported by the National Basic Research Program of China (2011CB707802), and the National High-Tech Program of China (2012AA011601).

References

1. Heemels, M.-T.: Ageing. Nature 464, 503 (2010)
2. Frisoni, G.B., Fox, N.C., Jack Jr., C.R., Scheltens, P., Thompson, P.M.: The clinical use of structural MRI in Alzheimer disease. Nature Reviews Neurology 6, 67–77 (2010)
3. Fan, Y., Batmanghelich, N., Clark, C.M., Davatzikos, C.: Spatial patterns of brain atrophy in MCI patients, identified via high-dimensional pattern classification, predict subsequent cognitive decline. Neuroimage 39, 1731–1743 (2008)
4. Franke, K., Ziegler, G., Kloppel, S., Gaser, C.: Estimating the age of healthy subjects from T1-weighted MRI scans using kernel methods: exploring the influence of various parameters. Neuroimage 50, 883–892 (2010)
5. Brickman, A.M., Habeck, C., Zarahn, E., Flynn, J., Stern, Y.: Structural MRI covariance patterns associated with normal aging and neuropsychological functioning. Neurobiol. Aging. 28, 284–295 (2007)
6. Wang, B., Pham, T.D.: MRI-based age prediction using hidden Markov models. J. Neurosci Methods 199, 140–145 (2011)
7. Brown, T.T., Kuperman, J.M., Chung, Y., Erhart, M., McCabe, C., et al.: Neuroanatomical Assessment of Biology Maturity. Current Biology 22, 1–6 (2012)
8. Taki, Y., Kinomura, S., Sato, K., Goto, R., Kawashima, R., et al.: A longitudinal study of gray matter volume decline with age and modifying factors. Neurobiol. Aging. 32, 907–915 (2009)
9. Salat, D.H., Lee, S.Y., van der Kouwe, A.J., Greve, D.N., Fischl, B., et al.: Age-associated alterations in cortical gray and white matter signal intensity and gray to white matter contrast. NeuroImage 48, 21–28 (2009)
10. Tisserand, D.J., van Boxtel, M.P.J., Pruessner, J.C., Hofman, P., Evans, A.C., et al.: A Voxel-based morphometric study to determine individual differences in gray matter density associated with age and cognitive change over time. Cereb. Cortex 14, 966–973 (2004)
11. Galluzzi, S., Beltramello, A., Filippi, M., Frisoni, G.B.: Aging. Neurol Sci. 29, s296–s300 (2008)
12. Ge, Y., Grossman, R.I., Babb, J.S., Rabin, M.L., Mannon, L.J., et al.: Age-related total gray matter and white matter changes in normal adult brain. Part I: volumetric MR Imaging analysis. Am J. Neuroradiol. 23, 1327–1333 (2002)
13. Giorgio, A., Santelli, L., Tomassini, V., Bosnell, R., Smith, S., et al.: Age-related changes in grey and white matter structure throughout adulthood. NeuroImage 51, 943–951 (2010)

14. Good, C.D., Johnsrude, I.S., Ashburner, J., Henson, R.N.A., Friston, K.J., et al.: A voxel-based morphometric study of ageing in 465 normal adult human brains. NeuroImage 14, 21–36 (2001)
15. Smith, C.D., Chebrolu, H., Wekstein, D.R., Schmitt, F.A., Markesbery, W.R.: Age and gender effects on human brain anatomy: A voxel-based morphometric study in healthy elderly. Neurobiol. Aging. 28, 1075–1087 (2007)
16. Shen, H., Wang, L., Liu, Y., Hu, D.: Discriminative analysis of resting-state functional connectivity patterns of schizophrenia using low dimensional embedding of fMRI. Neuroimage 49, 3110–3121 (2010)
17. Robinson, E.C., Hammers, A., Ericsson, A., Edwards, A.D., Rueckert, D.: Identifying population differences in whole-brain structural networks: a machine learning approach. Neuroimage 50, 910–919 (2010)
18. Su, L., Wang, L., Chen, F., Shen, H., Li, B., et al.: Sparse representation of brain aging: extracting covariance patterns from structural MRI. PLoS One 7, e36147 (2012)
19. Daubechies, I., Roussos, E., Takerkart, S., Benharrosh, M., Golden, C., et al.: Independent component analysis for brain fMRI does not select for independence. Proc. Natl. Acad. Sci. USA 106, 10415–10422 (2009)
20. Marcus, D.S., Wang, T.H., Parker, J., Csernansky, J.G., Morris, J.C., et al.: Open access series of imaging studies (OASIS): cross-sectional MRI data in young, middle aged, nondemented, and demented older adults. J. Cognitive NeuroSci. 19, 1498–1507 (2007)
21. Ashburner, J.: A fast diffeomorphic image registration algorithm. NeuroImage 38, 95–113 (2007)
22. Li, Y., Namburi, P., Yu, Z., Guan, C., Feng, J., et al.: Voxel selection in fMRI data analysis based on sparse representation. IEEE T. Bio.-Med. Eng. 56, 2439–2451 (2009)
23. Ecker, C., Rocha-Rego, V., Johnston, P., Mourao-Miranda, J., Marquand, A., et al.: Investigating the predictive value of whole-brain structural MR scans in autism: a pattern classification approach. Neuroimage 49, 44–56 (2010)
24. Fan, Y., Shen, D., Gur, R.C., Gur, R.E., Davatzikos, C.: COMPARE: classification of morphological patterns using adaptive regional elements. IEEE Trans. Med. Imaging 26, 93–105 (2007)
25. Duara, R., Loewenstein, D.A., Potter, E., Appel, J., Greig, M.T., et al.: Medial temporal lobe atrophy on MRI scans and the diagnosis of Alzheimer disease. Neurology 71, 1986–1992 (2008)
26. Li, S., Xia, M., Pu, F., Li, D., Fan, Y., et al.: Age-related changes in the surface morphology of the central sulcus. Neuroimage 58, 381–390 (2011)